Published in final edited form as:

J Immunol. 2017 August 01; 199(3): 911–919. doi:10.4049/jimmunol.1700595.

Differential requirements for Tcf1 long isoforms in CD8+ and CD4+ T cell responses to acute viral infection

Jodi A. Gullicksrud[1,2], **Fengyin Li**[1], **Shaojun Xing**[1], **Zhouhao Zeng**[3], **Weiqun Peng**[3], **Vladimir P. Badovinac**[1,2,4], **John T Harty**[1,2], and **Hai-Hui Xue**[1,2,5]

[1]Department of Microbiology, Carver College of Medicine, University of Iowa, Iowa City, IA 52242

[2]Interdisciplinary Immunology Graduate Program, University of Iowa, Iowa City, IA 52242

[3]Department of Physics, The George Washington University, Washington DC, 20052

[4]Department of Pathology, Carver College of Medicine, University of Iowa, Iowa City, IA 52242

Abstract

In response to acute viral infections, activated naïve T cells give rise to effector T cells that clear the pathogen and memory T cells that persist long-term and provide heightened protection. T cell factor 1 (Tcf1) is essential for several of these differentiation processes. Tcf1 is expressed in multiple isoforms, with all isoforms sharing the same HDAC and DNA-binding domains, and the long isoforms containing a unique N-terminal β-catenin-interacting domain. Here we specifically ablated Tcf1 long isoforms in mice, while retaining expression of Tcf1 short isoforms. During $CD8^+$ T cell responses, Tcf1 long isoforms were dispensable for generating cytotoxic $CD8^+$ effector T cells and maintaining memory $CD8^+$ T cell pool size, but contributed to optimal maturation of central memory $CD8^+$ T cells and their optimal secondary expansion in a recall response. On the other hand, Tcf1 long isoforms were required for differentiation of T follicular helper (T_{FH}) cells but not T helper 1 (T_H1) effectors elicited by viral infection. Whereas Tcf1 short isoforms adequately supported Bcl6 and ICOS expression in T_{FH} cells, Tcf1 long isoforms remained important for suppressing the expression of Blimp1 and T_H1-associated genes and for positively regulating Id3 to restrain germinal center T_{FH} cell differentiation. Furthermore, formation of memory T_H1 and memory T_{FH} cells strongly depended on Tcf1 long isoforms. These data reveal that Tcf1 long and short isoforms have distinct yet complementary functions and may represent an evolutionarily conserved means to ensure proper programming of $CD8^+$ and $CD4^+$ T cell responses to viral infection.

In response to a viral infection, naïve T cells that recognize their cognate antigens become activated, expand prolifically, and differentiate into effector T cells equipped with diverse functions. Effector $CD8^+$ T cells acquire cytotoxic functions and eliminate virus-infected cells (1, 2). On the other hand, activated $CD4^+$ T cells predominantly differentiate into two types of effectors, T helper 1 (T_H1) cells that secrete interferon-γ (IFN-γ) and enhance the cytotoxicity of effector $CD8^+$ T cells, or T follicular helper (T_{FH}) cells that secret IL-4 and IL-21 and provide essential help to antibody-producing B cells (3–5). Effector T cells are

[5]Corresponding author: Hai-Hui Xue, 51 Newton Rd. BSB 3-772, Iowa City, IA 52242, Tel: 319-335-7937, Fax: 319-335-9006, hai-hui-xue@uiowa.edu.

heterogeneous and contain subsets that have different kinetics of contraction following the peak responses, and hence different potential to give rise to memory T cells. Whereas memory $CD8^+$ T cells are more durable than memory $CD4^+$ T cells, both populations contribute to enhanced responses upon re-challenge with the same antigen.

Differentiation of effector T cells and their transition to memory T cells are coordinated by transcriptional regulators (6). In activated $CD8^+$ T cells, T-bet and Blimp1 transcription factors as well as the Id2 cofactor are potently induced, and critically regulate $CD8^+$ effector cell differentiation and acquisition of cytotoxic functions (7–9). On the other hand, Eomes, Bcl6, and Id3 promote the transition and survival of memory $CD8^+$ T cells (9–11). In $CD4^+$ T cells, T-bet and Bcl6 are the lineage-specifying master regulator for T_H1 and T_{FH} cells, respectively (3, 4), and induction of Blimp1 and Id2 favors T_H1 differentiation at the expense of T_{FH} lineage (12, 13). In contrast to advances in elucidating the transcriptional networks in $CD4^+$ lineage differentiation at the effector phase, little is known about transcriptional regulation involved in memory $CD4^+$ T cell formation and functions.

T cell factor 1 (Tcf1) has been known as a transcription factor acting downstream of the Wnt pathway and can interact with β-catenin coactivator. β-catenin is post-translationally regulated and stabilized by Wnt- or prostaglandin-derived signals. In addition to its essential role for T cell development (14, 15), recent studies have revealed that Tcf1 critically regulates mature T cell responses. Whereas loss of Tcf1 modestly diminished production of effector $CD8^+$ T cells, Tcf1 is essential for maturation, longevity, and secondary expansion of memory $CD8^+$ T cells (16, 17). In activated $CD4^+$ T cells, Tcf1 appears to restrain T_H1 differentiation *in vitro* (18) but is essential for activating the T_{FH} program by acting upstream of Bcl6 (12, 19, 20). Due to differential promoter usage and alternative splicing, multiple Tcf1 isoforms can be detected in T cells (21). All isoforms contain a C-terminal HMG DNA binding domain, which can also interact with Groucho/Transducin-like Enhancer-of-split (TLEs) corepressor proteins, and a newly discovered HDAC domain (22). The Tcf1 long isoforms (p45 and p42) contain an N-terminal β-catenin-binding domain, while the Tcf1 short isoforms (p33 and p30) lack this domain and hence cannot interact with β-catenin. Most of the previous loss-of-function studies ablated all Tcf1 isoforms. The specific requirements for the Tcf1 long isoforms in effector and memory T cell responses have not yet been elucidated.

Here we specifically ablated Tcf1 long isoforms in mouse, and coupled this model with MHC-I- and MHC-II-restricted T cell receptor (TCR) transgenes to dissect the roles of Tcf1 isoforms in regulating mature $CD8^+$ and $CD4^+$ T cell responses. Our data showed that Tcf1 long isoforms were dispensable for generation of cytotoxic $CD8^+$ effector T cells and helper T_H1 cells in response to viral infection, while Tcf1 short isoforms were sufficient for maintaining memory $CD8^+$ T cell pool size. On the other hand, Tcf1 long isoforms remained critical for T_{FH} differentiation at the effector phase and for generation of both memory T_H1 and memory T_{FH} cells. This study reveals a functional complementation among Tcf1 isoforms in programming mature T cell responses, and further suggests an inter-isoform coordination is necessary to constitute a fully functional gene product.

Materials and Methods

Mice

$p45^{+/GFP}$ (*i.e.*, $p45^{+/-}$) mice were generated as previously described (23), and cross-bred with P14 or SMARTA TCR transgenes to generate P14 $p45^{-/-}$ or SMARTA $p45^{-/-}$ mice, respectively. Our recent analysis of thymocyte development in the p45-targeted mice showed no detectable differences between $p45^{+/+}$ and $p45^{+/-}$ animals (23), suggesting that heterozygosity of the p45-targeted allele does not significantly impact T cell biology. As such, we used T cells from $p45^{+/-}$ mice as controls in this study, and the Tcf1-EGFP reporter embedded in the $p45^{+/-}$ allele was utilized to mark Tcf1 expression in $CD4^+$ and $CD8^+$ T cells at different stages of responses to viral infection. C57BL/6J and B6.SJL mice were from the Jackson Laboratory. All mice analyzed were 6–12 weeks of age, and both genders are used without randomization or blinding. All mouse experiments were performed under protocols approved by the Institutional Animal Use and Care Committees of the University of Iowa.

Flow cytometry

Single-cell suspensions were prepared from the spleen, lymph nodes (LNs), or peripheral blood lymphocytes (PBLs), and surface or intracellularly stained as described (19). The fluorochrome-conjugated antibodies were as follows: anti-CD8 (53-6.7), anti-CD4 (RM4-5), anti-CD44 (IM7), anti-CD62L (MEL-14), anti-PD-1 (J43), anti-CD45.1 (A20), anti-CD45.2 (104), anti-ICOS (C398.4A), anti-IFN-γ (XMG1.2), anti-TNFα (MP6-XT22), anti-Eomes (Dan11mag), anti-T-bet (eBio4B10), anti-IL-2 (JES6-5H4), anti-IL-7Rα (eBio17B7) and anti-KLRG1 (2F1) from eBiosciences; anti-Bcl6 (K112-91) from BD Biosciences; anti-human granzyme B (FGB12) and corresponding isotype control from Invitrogen/Life Technologies, anti-SLAM (TC15-12F12.2) from BioLegend. For detection of CXCR5, three-step staining protocol was used with unconjugated anti-CXCR5 (2G8; BD Biosciences) (24). For detection of Bcl6, surface-stained cells were fixed and permeabilized with the Foxp3/Transcription Factor Staining Buffer Set (eBiosciences), followed by incubation with a fluorochrome-conjugated antibody or isotype control. Peptide-stimulated cytokine production and detection by intracellular staining were as described (25). Data were collected on a FACSVerse (BD Biosciences) and were analyzed with FlowJo software (TreeStar).

Adoptive transfer and viral infection

Naïve $CD45.2^+$ P14 $CD8^+$ T cells or SMARTA $CD4^+$ T cells were isolated from the LNs of P14- or SMARTA-transgenic $p45^{+/-}$ or $p45^{-/-}$ mice. For characterization of $CD8^+$ T cell responses, 2×10^4 $Vα2^+$ P14 $CD8^+$ T cells were intravenously (*i.v.*) injected into $CD45.1^+$ B6.SJL recipient mice and infected intraperitoneally (*i.p*) with 2×10^5 PFU of lymphocytic choriomeningitis virus, Armstrong strain (LCMV-Arm). For characterization of $CD4^+$ T cell responses, 2×10^5 $Vα2^+$ SMARTA $CD4^+$ T cells were *i.v.* injected into $CD45.1^+$ hosts and infected similarly. For examining $CD4^+$ T cell responses under a competitive condition, 5,000 $p45^{+/-}$ or $p45^{-/-}$ SMARTA $CD4^+$ T cells were mixed with the same number of WT $CD45.1^+CD45.2^+$ SMARTA $CD4^+$ T cells and adoptively transferred. At ≥ 40 *dpi*, the

immune mice were *i.v.* infected with 2×10^6 PFU of LCMV clone 13 (Cl13) to elicit secondary $CD8^+$ or $CD4^+$ T cell responses.

Immunoblotting

$CD44^{lo}CD62L^+$ naïve P14 $CD8^+$ T cells or SMARTA $CD4^+$ T cells were sort-purified from the spleens of P14- or SMARTA-transgenic $p45^{+/-}$ or $p45^{-/-}$ mice. Cell lysates were prepared from the sorted cells, resolved on SDS-PAGE, and immunoblotted with an anti-Tcf1 antibody (C46C7, Cell Signaling Technologies) as previously described (23).

RNA-Seq and quantitative RT-PCR

$p45^{+/-}$ or $p45^{-/-}$ SMARTA $CD4^+$ T cells were adoptively transferred and recipients infected as described above. On 8 *dpi*, PD-1^{lo} $CXCR5^+$ cells were sort-purified from $CD45.2^+CD4^+$ splenocytes. The total RNA was extracted and subjected to RNA-Seq analysis as previously described (19). The RNA-Seq data were deposited at the Gene Expression Omnibus (GEO) under the accession number GSE98347 (https://www.ncbi.nlm.nih.gov/geo/query/acc.cgi?acc=gse98347). For validation of key gene expression changes, the RNA was reverse-transcribed and analyzed by quantitative PCR as previously described (19). The primers used for *Id2* were 5′-catcagcatcctgtccttgc and 5′-gtgttctcctggtgaaatgg, and those for *Id3* were 5′-atctcccgatccagacagc and 5′-gagagagggtcccagagtcc.

Chromatin immunoprecipitation (ChIP)

WT SMARTA $CD4^+$ T cells were adoptively transferred and recipients infected as above. On 8 *dpi*, $CXCR5^-SLAM^{hi}$ T_H1 and $CXCR5^+SLAM^{lo}$ T_{FH} cells were sort-purified from $CD45.2^+CD4^+$ splenocytes and cross-linked, and the resulting chromatin fragments were immunoprecipitated with an anti-Tcf1 antibody (C46C7) or normal rabbit IgG, as previously described (19). Enriched Tcf1 binding at the *Id3* transcription start site was determined by quantitative PCR.

Statistical analyses

Data from multiple experiments were analyzed with Student's *t*-test with two-tailed distribution, assuming equal sample variance when $p>0.05$ on F-test. When $p \leq 0.05$ on F-test comparing the variances, Welch's correction was applied.

Results

Tcf1 long isoforms are dispensable for $CD8^+$ effector T cell differentiation

Tcf1 proteins are encoded by the *Tcf7* gene, with long isoforms produced from transcripts initiated at exon 1 and short isoforms from transcripts initiated at exon 3. Previously we have generated a Tcf1-EGFP reporter mouse strain, where we inserted an IRES-EGFP cassette into the first intron of *Tcf7* gene (26). In front of the cassette, we placed an En2 splice acceptor that forced the splicing of exon 1 to this cassette instead of exon 2. Mice homozygous for the Tcf1-EGFP reporter alleles thus failed to produce Tcf1 long isoforms, p45 and p42; for simplicity, this strain is called $p45^{-/-}$ herein. To assess the importance of Tcf1 long isoforms (p45 and p42) in $CD8^+$ T cell responses to viral infection, we crossed

$p45^{-/-}$ mice with the P14 TCR transgene, which encodes a TCR specific for the glycoprotein (GP) 33 epitope of LCMV. As expected, $p45^{-/-}$ P14 $CD8^+$ T cells were deficient for Tcf1 long isoforms but retained the expression of Tcf1 short isoforms, albeit at a reduced amount (Fig. 1A). Loss of Tcf1 long isoforms moderately reduced the frequency of P14 $CD8^+$ T cells in the LNs, but did not result in aberrant activation of peripheral $CD8^+$ T cells, as determined by the $CD62L^{hi}$ phenotype (Fig. 1B).

To facilitate functional characterization on a per cell basis, we adoptively transferred the same numbers (2×10^4) of $p45^{+/-}$ or $p45^{-/-}$ P14 $CD8^+$ T cells into congenic recipients followed by infection with LCMV-Arm. As tracked in PBLs, both $p45^{+/-}$ and $p45^{-/-}$ $CD45.2^+$ $CD8^+$ effector T cells showed similar frequency among antigen-experienced $CD11a^{hi}CD8^{int}$ T cells (Fig. 1C). In the spleens, similar numbers of $p45^{+/-}$ and $p45^{-/-}$ $CD45.2^+CD8^+$ effector T cells were generated at the peak response, *i.e.*, 8 days post-infection (*dpi*) (Fig. 1D). By comparison, loss of all Tcf1 isoforms diminishes $CD8^+$ effector T cells by approximately 50% in both PBLs and spleens (16). $CD8^+$ effector T cells are heterogeneous, with $KLRG1^{hi}CD127^-$ cells as terminally differentiated effector $CD8^+$ T cells, and the $KLRG1^{lo}CD127^+$ subset showing increased potential to give rise to memory $CD8^+$ T cells (6). As observed in $p45^{+/-}$ $CD8^+$ T cells, the Tcf1-EGFP reporter expression is potently diminished in $KLRG1^{hi}CD127^-$ cells, but partially retained in the $KLRG1^{lo}CD127^+$ subset (Fig. 1E). This is consistent with our previous observations that Tcf1 and Lef1 are required for generation of the $KLRG1^{lo}CD127^+$ subset (27). However, the $KLRG1^{lo}CD127^+$ subset in $p45^{-/-}$ $CD8^+$ effectors was only modestly reduced in frequency and numbers (Fig. 1F). Both $p45^{+/-}$ and $p45^{-/-}$ $CD8^+$ effectors exhibited similar capacity to produce IFN-γ, TNF-α, and granzyme B (Fig. 1G–1H), and by comparison, these functional aspects are not affected by loss of all Tcf1 isoforms as shown in our previous study (16). Collectively, these data indicate that Tcf1 long isoforms are dispensable for clonal expansion and cytotoxic functions of $CD8^+$ effector T cells.

Tcf1 long isoforms contribute to maturation of central memory $CD8^+$ T cells

Following the peak response to LCMV infection, $p45^{+/-}$ and $p45^{-/-}$ $CD45.2^+CD8^+$ effector T cells contracted similarly (Fig. 1C), and at ≥ 60 *dpi*, similar numbers of $p45^{+/-}$ and $p45^{-/-}$ memory $CD8^+$ T cells were found in the recipient spleens (Fig. 2A). Memory $CD8^+$ T cells in the secondary lymphoid organs are heterogeneous, with the $CD62L^-$ subset as effector memory (T_{EM}) cells that reside in non-lymphoid tissues, and the $CD62L^+$ subset as central memory (T_{CM}) cells that are capable of self-renewal and conferring long-term protection (28). Compared with $CD8^+$ effector T cells, most of the memory $CD8^+$ T cells upregulated Tcf1, and the $CD62L^+$ subset expressed higher levels of Tcf1 as determined by the Tcf1-EGFP reporter activity (Fig. 2B, compare with Fig. 1E). Our previous studies showed that deletion of all Tcf1 isoforms almost completely abrogated generation of $CD62L^+$ T_{CM} cells and caused substantial decrease in Eomes expression (16). In $p45^{-/-}$ memory $CD8^+$ T cell pool, $CD62L^+$ cells were generated, but at diminished frequency and numbers (Fig. 2C). In addition, $p45^{-/-}$ memory $CD8^+$ T cells showed modest reduction in Eomes expression, accompanied by a modest increase in T-bet expression (Fig. 2D). Regarding functional aspects, fewer $p45^{-/-}$ memory $CD8^+$ T cells (in both $CD62L^-$ and $CD62L^+$ subsets) were capable of producing IL-2 than $p45^{+/-}$ cells (Fig. 2E), whereas they showed similar

production of IFN-γ and TNF-α (data not shown). Additionally, $p45^{-/-}$ memory $CD8^+$ T cells showed modest increase in granzyme B compared with $p45^{+/-}$ cells (Fig. 2F). These observations indicate that loss of Tcf1 long isoforms does not affect the pool size of memory $CD8^+$ T cells but predisposes them to a T_{EM} phenotype.

To assess the recall response by memory $CD8^+$ T cells, we re-challenged the immune recipient mice with LCMV-Cl13. As detected on day 5 post-infection, both $p45^{+/-}$ and $p45^{-/-}$ memory $CD8^+$ T cells underwent substantial secondary expansion, although the numbers of $p45^{-/-}$ secondary $CD8^+$ effector T cells in the spleens were modestly decreased (Fig. 2G), which is in contrast to severely impaired secondary expansion in the absence of all Tcf1 isoforms (16). Similar to $CD8^+$ effector T cells in the primary response, the secondary $CD8^+$ effector T cells were heterogeneous, with the $KLRG1^{lo}CD127^+$ subset retaining substantially higher Tcf1-EGFP reporter activity than the $KLRG1^{hi}CD127^-$ subset (Fig. 2H). Loss of Tcf1 long isoforms did not detectably perturb the subset composition or IFN-γ and TNF-α production in the secondary effectors (Fig. 2H and data not shown). Collectively, these data suggest that Tcf1 long isoforms contribute to optimal maturation of T_{CM} cells and optimal secondary expansion in a recall response. It is also noteworthy that reduced expression of Tcf1 short isoforms in $p45^{-/-}$ $CD8^+$ T cells may also be a contributing factor.

Tcf1 long isoforms are required for T_{FH} differentiation at the effector phase of $CD4^+$ T cell responses

We and others have recently demonstrated that deletion of all Tcf1 isoforms impairs T_{FH} differentiation in response to viral infections (12, 19, 20). To determine the requirements for Tcf1 long isoforms during $CD4^+$ T cell responses, we crossed the $p45^{-/-}$ strain with SMARTA TCR transgene, which encodes a TCR specific for the GP61 epitope of LCMV. By immunoblotting, we validated that $p45^{-/-}$ SMARTA $CD4^+$ T cells were deficient for Tcf1 long isoforms but retained the expression of Tcf1 short isoforms, also at a reduced amount (Fig. 3A). Although the frequency of SMARTA $CD4^+$ T cells in the LNs was diminished in $p45^{-/-}$ mice, the majority of $p45^{-/-}$ SMARTA $CD4^+$ T cells exhibited a $CD44^{lo}CD62L^{hi}$ phenotype, suggesting that loss of Tcf1 long isoforms did not result in aberrant activation of peripheral $CD4^+$ T cells (Fig. 3B).

To investigate the regulatory roles of Tcf1 long isoforms on a per cell basis, we adoptively transferred the same numbers (2×10^5) of $p45^{+/-}$ or $p45^{-/-}$ SMARTA $CD4^+$ T cells from LNs into congenic recipients followed by infection with LCMV-Arm. At the peak of effector $CD4^+$ T cell responses (*i.e.*, 8 *dpi*), $p45^{+/-}$ and $p45^{-/-}$ SMARTA $CD4^+$ T cells expanded to similar levels, showing similar frequency and numbers of effector $CD4^+$ T cells in the spleen of recipient mice (Fig. 3C). Viral infection elicits two major forms of effector $CD4^+$ T cells, T_H1 and T_{FH} cells, which exhibit $CXCR5^-SLAM^{hi}$ and $CXCR5^+SLAM^{lo}$ phenotypes, respectively. $p45^{+/-}$ effector $CD4^+$ T cells contained approximately equal amounts of T_H1 and T_{FH} cells; in contrast, $p45^{-/-}$ effector $CD4^+$ T cells were strongly skewed toward the T_H1 phenotype (Fig. 3D). As a result, $p45^{-/-}$ SMARTA $CD4^+$ T cells generated markedly fewer T_{FH} cells than the $p45^{+/-}$ counterparts (Fig. 3D), similar to T_{FH} differentiation defects observed in the absence of all Tcf1 isoforms (12, 19, 20). On the other hand, both $p45^{-/-}$ and

p45$^{+/-}$ SMARTA CD4^{+} T cells gave rise to similar amounts of effector T_H1 cells (Fig. 3D). These data suggest that Tcf1 long isoforms are important in directing effective T_{FH} differentiation, but are dispensable for T_H1 responses.

In the experiments above, we transferred a relatively large number of SMARTA CD4^{+} T cells so as to obtain sufficient cells for RNA-Seq and memory phase analysis (see below). To exclude a secondary impact derived from a higher precursor frequency and demonstrate an intrinsic requirement for Tcf1 long isoforms, we transferred a small number of p45$^{+/-}$ or p45$^{-/-}$ SMARTA CD4^{+} T cells in a competitive setting. Specifically, we mixed CD45.2^{+} p45$^{+/-}$ or p45$^{-/-}$ SMARTA CD4^{+} T cells (as test cells) with the same number of CD45.1^{+}CD45.2^{+} wild-type (WT) SMARTA CD4^{+} T cells (as competitors) (Fig. 4A). We then adoptively transferred a total of 10,000 SMARTA CD4^{+} T cells (5,000 each of test cells and competitors) into CD45.1^{+} recipients, followed by LCMV-Arm infection. On 8 *dpi*, within the T_H1 compartment, the p45$^{+/-}$:WT ratio was largely maintained at 1:1, and the p45$^{-/-}$:WT ratio was modestly decreased (Fig. 4B–4C). Within the T_{FH} cells, however, the p45$^{-/-}$:WT ratio was reduced by >5 fold compared with the p45$^{+/-}$:WT ratio (Fig. 4B–4C). Thus, analysis under the competitive setting at a lower precursor frequency further corroborated a specific, intrinsic requirement for Tcf1 long isoforms in T_{FH} differentiation.

Tcf1 long isoforms regulate a unique subset of genes in the Tfh program

We previously showed that Tcf1 critically regulates activation of the T_{FH} program in primed CD4^{+} T cells, and deletion of all Tcf1 isoforms diminishes the expression of Bcl6 and ICOS (19). However, p45$^{+/-}$ and p45$^{-/-}$ T_{FH} cells showed similar Bcl6 and ICOS expression (Fig. 5A–5B), suggesting that Tcf1 short isoforms are sufficient for supporting Bcl6 and ICOS induction, in spite of reduced protein expression. T_{FH} differentiation is known as a step-wise process (4), with T_{FH} lineage-committed cells undergoing further maturation and becoming germinal center (GC)-T_{FH} cells, as marked by high PD-1 expression. Although there was an overall reduction of p45$^{-/-}$ T_{FH} cells, PD-1^{hi}CXCR5^{+} GC-T_{FH} cells were detected at similar frequency and numbers in p45$^{+/-}$ and p45$^{-/-}$ effector SMARTA CD4^{+} T cells (Fig. 5C). Thus, loss of Tcf1 long isoforms showed stronger impact on non-GC-T_{FH} cells, causing subset composition changes within the T_{FH} population. By comparison, both non-GC T_{FH} and GC T_{FH} cells were diminished in the absence of all T cell isoforms (19). Therefore, Tcf1 short isoforms appears to be adequate for promoting GC-T_{FH} maturation.

To search for downstream genes that account for defective p45$^{-/-}$ T_{FH} differentiation, we specifically sorted p45$^{+/-}$ and p45$^{-/-}$ PD-1^{lo} CXCR5^{+}, non-GC-T_{FH} cells on 8 *dpi* and performed RNA-Seq analysis. By a setting of ≥ 2 fold expression changes and false discovery rate (FDR) q value <0.05, we found 89 downregulated and 119 upregulated genes in p45$^{-/-}$ T_{FH} cells compared with p45$^{+/-}$ counterparts (Supplemental Table 1). Transcriptomic changes have been profiled in T_{FH} cells lacking all Tcf1 isoforms or both Tcf1 and Lef1 proteins (19, 20). Whereas differences in specific cell subsets analyzed and profiling platforms utilized among these studies prevented a meaningful and fair comparison for specific genes affected, the number of differentially expressed genes was substantially lower in p45$^{-/-}$ T_{FH} cells than that found in Tcf1/Lef1-deficient T_{FH} cells, suggesting a relatively limited impact of deficiency in Tcf1 long isoforms on T_{FH} transcriptome.

Functional annotation using the DAVID Bioinformatics Resources revealed a partial activation of T_H1 program in $p45^{-/-}$ T_{FH} cells, including upregulation of *Prdm1*, *Il2ra*, and *Ifng* (encoding Blimp1 transcription factor, CD25, and IFN-γ, respectively) (Fig. 5D). Increased expression of *Prdm1* was validated by quantitative RT-PCR (Fig. 5G). Blimp1 is known to promote activated $CD4^+$ T cells to a T_H1 fate at the expense of T_{FH} differentiation (29), and Tcf1 and Bcl6 co-occupy an intron 3 regulatory region in the *Prdm1* gene locus (19, 30). Our data suggest that Tcf1 long isoforms are critical in repressing the T_H1 potential in T_{FH} cells.

Among the upregulated genes included *Maf*, *Fos* and *Fosb* (Fig. 5E). Maf is necessary for promoting T_{FH} differentiation and inducing IL-21 (31, 32). AP-1 factors including Fos and FosB may contribute to recruiting Bcl6 to its target genes in T_{FH} cells (30). Among the downregulated genes, a prominent subset was involved in transcriptional regulation, including *Irf6*, *Nfe2*, *Sox4*, and *Id3* (Fig. 5F). Importantly, the first three genes were detected at low abundance in T_{FH} cells (< 5 FPKMs); in contrast, *Id3* was highly abundant in T_{FH} cells (132 PFKMs on average). As validated in Fig. 5G, *Id3* expression was diminished in $p45^{-/-}$ T_{FH} cells, whereas *Id2* was not detectably altered. By chromatin immunoprecipitation, we further found that Tcf1 exhibited enriched binding to the transcription start site of *Id3* gene in T_{FH} cells but not T_H1 cells (Fig. 5H), establishing *Id3* as a direct target gene of Tcf1 in T_{FH} cells. It has been recently shown that Id3 deficiency results in evident accumulation of GC-T_{FH} cells (13). These data collectively suggest that another important function of Tcf1 long isoforms appears to be restraining GC-T_{FH} differentiation by positive regulation of Id3, maybe aided by suppression of Maf and AP-1 factors.

Tcf1 long isoforms are essential for formation of memory T_H1 and T_{FH} cells

We continued to track the SMARTA $CD4^+$ T cell responses at the memory phase, *i.e.*, > 40 *dpi*, and found significantly fewer $p45^{-/-}$ memory $CD4^+$ T cells than the $p45^{+/-}$ counterparts (Fig. 6A). Compared with $CD4^+$ effector T cells, the number of $p45^{+/-}$ memory $CD4^+$ T cells was a result of approximately 20-fold contraction; in contrast, the number of $p45^{-/-}$ memory $CD4^+$ T cells represented an almost 200-fold contraction of corresponding $CD4^+$ effector T cells (Fig. 6B). Phenotypic analysis using SLAM and CXCR5 expression further revealed that $p45^{-/-}$ memory $CD4^+$ T cells were strongly skewed toward T_H1, with very few $SLAM^{lo}CXCR5^+$ memory T_{FH} cells detected (Fig. 6C). In spite of the lineage bias in the absence of Tcf1 long isoforms, $p45^{-/-}$ memory T_H1 and T_{FH} cells both showed more potent contraction than their the $p45^{+/-}$ counterparts (Fig 6C). As detected by the Tcf1-GFP reporter in $p45^{+/-}$ $CD4^+$ T cells, although Tcf1 was downregulated in T_H1 effectors, it was upregulated in memory T_H1 cells, whereas Tcf1-GFP reporter was detected at high levels in both effector and memory T_{FH} cells (Fig. 6D). We next assessed the recall response by memory $CD4^+$ T cells, by re-challenging the immune recipient mice with LCMV-Cl13. As detected on day 5 post-infection, $p45^{-/-}$ secondary $CD4^+$ effectors were greatly diminished in numbers and remained strongly skewed toward T_H1 cells, containing very few T_{FH} cells (Fig. 6E). These data suggest that Tcf1 long isoforms are essential for generation of memory T_H1 as well as memory T_{FH} cells and ensuing secondary responses. It should be noted that

reduced expression of Tcf1 short isoforms in $p45^{-/-}$ $CD4^+$ T cells may also have contributed to defects in memory $CD4^+$ T cells.

DISCUSSION

Tcf1 is known for its versatile functions in regulating T cell development and mature $CD8^+$ and $CD4^+$ T cell responses to infections (15, 33). Most of the previous studies involved deletion of all Tcf1 isoforms. Until recently, Tcf1 short isoforms were generally considered to function as dominant negatives for the full-length molecule, due to their inability to interact with the co-activator β-catenin. Using a new mouse model where generation of transcripts for Tcf1 long isoforms was abrogated, we achieved specific retention of Tcf1 short isoforms only. We have recently showed that Tcf1 short isoforms are sufficient to support developing thymocytes to traverse through maturation stages without causing obvious developmental blocks, whereas Tcf1 long isoforms remain necessary for optimal thymic survival (23). Coupled with MHC-I- or MHC-II-restricted TCR transgenes, we employed the Tcf1 long isoform-targeted mice to reveal isoform-specific requirements for $CD8^+$ and $CD4^+$ T cell differentiation in response to viral infection.

At the peak of $CD8^+$ T cell response to LCMV, the terminally differentiated $KLRG1^{hi}CD127^-$ $CD8^+$ effector T cells exhibit strong downregulation of all Tcf1 isoforms. It is therefore not surprising that loss of Tcf1 long isoforms did not show a detectable impact on the numbers or functions of $CD8^+$ effector T cells. Recent studies examined early events of $CD8^+$ T cell activation *in vivo* and found that Tcf1 expression is retained at high levels in all daughter cells during the first 3–4 divisions. In the ensuing divisions, due to asymmetrical signaling *via* the PI3K pathway, most daughter cells obliterate Tcf1 expression and become differentiated $CD8^+$ effector T cells, while some daughter cells maintain higher Tcf1 expression, acquire ‘self-renewal’ capacity, and give rise to memory $CD8^+$ T cells (34, 35). In this scenario, retention of Tcf1 short isoforms only appears to be adequate to maintain the self-renewing $Tcf1^{hi}$ population in spite of diminished amount of protein expression because the memory $CD8^+$ T cell pool was similar between $p45^{+/-}$ and $p45^{-/-}$ genotypes. It is currently unknown if the $Tcf1^{hi}$ population at the effector phase is responsible for generation of both T_{EM} and T_{CM} cells. Loss of all Tcf1 isoforms almost completely abrogated T_{CM} maturation (16); in contrast, $p45^{-/-}$ T_{CM} cells were indeed generated, albeit at a modestly lower frequency. These data suggest that Tcf1 long isoforms remain necessary to promote optimal T_{CM} maturation.

Similar to the terminally differentiated $CD8^+$ effector T cells, $CXCR5^-SLAM^{hi}$ T_H1 cells at the effector phase of $CD4^+$ T cell responses potently downregulated Tcf1 expression, and loss of Tcf1 long isoforms was rather inconsequential for generation of T_H1 effectors. Unlike memory $CD8^+$ T cells which were unaffected in numbers by loss of Tcf1 long isoforms, $p45^{-/-}$ memory T_H1 cells were greatly diminished. It has also been shown that after 4–5 divisions during early $CD4^+$ T cell activation, Tcf1 expression is specifically retained in a subset of activated $CD4^+$ T cells due to asymmetrical signaling (36). The $Tcf1^{hi}$ $CD4^+$ cells seem to possess ‘self-renewal’ capacity as well, although whether they are direct precursors of memory $CD4^+$ T cells remains to be conclusively demonstrated. Nonetheless, formation of memory T_H1 cells is strongly dependent on Tcf1 long isoforms.

Another major $CD4^+$ T cell response to viral infection is differentiation to T_{FH} lineage, and deletion of all Tcf1 isoforms severely impairs generation of T_{FH} and GC-T_{FH} cells due to insufficient induction of Bcl6 and ICOS (12, 19, 20). This study shows that loss Tcf1 long isoforms greatly diminished the total number of T_{FH} cells but only modestly affected GC-T_{FH} cells. Transcriptomic analysis, coupled with phenotypic characterization, revealed that ablating Tcf1 long isoforms had a rather limited impact on the gene expression profile of T_{FH} cells compared with deleting all Tcf1 isoforms, similar to what we have observed in early thymocytes (23). Apparently, Tcf1 short isoforms, even at a reduced amount of protein, appeared to be sufficient to support induction of Bcl6 and ICOS in T_{FH} cells. Differentiation of non-GC T_{FH} to GC T_{FH} is a controlled process, and a recent study identified Id3 as a restraining factor (13). Our data demonstrated that Tcf1 directly binds to the *Id3* gene locus and Tcf1 short isoforms alone are not sufficient to support optimal Id3 expression in T_{FH} cells. Paradoxically, $p45^{-/-}$ T_{FH} cells upregulated Maf, another key T_{FH} regulator, and AP-1 factors which potentially cooperate with Bcl6. These gene expression changes may all indirectly contribute to promoting GC-T_{FH} differentiation, in addition to direct activation of Bcl6 transcription by Tcf1 itself. $p45^{-/-}$ T_{FH} cells also exhibited inappropriate activation of T_H1-associated genes, including *Prdm1, Il2ra* and *Ifng*, indicating another unique requirement for Tcf1 long isoforms in protecting the T_{FH} lineage integrity (37).

Recent studies have provided strong evidence that T_H1 and T_{FH} cells are largely committed to respective lineages at both effector and memory phases (38, 39). Loss of Tcf1 long isoforms not only impaired T_{FH} differentiation at the effector phase of $CD4^+$ T cell responses, but also caused a stronger contraction, resulting in even fewer memory T_{FH} cells. It has been suggested that stronger TCR stimulation during $CD4^+$ effector differentiation is associated with predisposition to form memory $CD4^+$ T cells (40). An increased strength of TCR signaling, resulting from extended dwell time of TCR with peptide-MHC II complex, is considered to favor T_{FH} differentiation (41). Since both memory $CD4^+$ T cells and T_{FH} differentiation were affected by loss of Tcf1 long isoforms, an interesting possibility is that Tcf1 may contribute to regulation of TCR signaling outcome, albeit not affecting TCR avidity or dwell time *per se*. In light of our recent finding that Tcf1 has intrinsic HDAC activity (22), Tcf1 may have global impact on the epigenome of T cells and hence affect their response to external stimuli. This scenario merits further investigation.

Collectively, our study identified differential requirements for Tcf1 long and short isoforms in mature $CD8^+$ and $CD4^+$ T cell responses. It is of interest to note the expression levels of Tcf1 short isoforms in $p45^{-/-}$ cells were modestly reduced compared with those in control cells. In spite of this, the Tcf1 short isoforms were adequate in supporting the memory $CD8^+$ T cell pool and induction of Bcl6 and ICOS in T_{FH} cells, indicating a positive regulatory role rather than being merely dominant negatives. On the other hand, Tcf1 long isoforms, plus appropriate amount of short isoforms, remained important for supporting T_{FH} differentiation at the effector phase and memory T_H1 and T_{FH} formation. It remains unknown if the defects associated with $p45^{-/-}$ cells are solely ascribed to lack of interaction with β-catenin. Nevertheless, our study supports a notion that generation of multiple isoforms from one gene may represent an evolutionarily conserved, fail-safe mechanism to ensure preservation of key biological functions.

Supplementary Material

Refer to Web version on PubMed Central for supplementary material.

Acknowledgments

This study is supported by grants from the NIH (AI112579 and AI115149 to HHX, AI042767 to JTH, AI119160 to HHX and VPB, AI114543 and GM113961 to VPB, AI121080 to HHX and WP, AI113806 to WP) and the US Department of Veteran Affairs (I01 BX002903 to HHX). JAG is a recipient of the University of Iowa Presidential Graduate Research Fellowship, T32 Pre-doctoral Training Grant in Immunology (AI007485), and the Ballard and Seashore Dissertation Fellowship. The flow cytometry core facility at the University of Iowa is supported by the Carver College of Medicine, Holden Comprehensive Cancer Center, and Iowa City Veteran's Administration Medical Center, and also by grants from the NCI (P30CA086862) and the National Center for Research Resources of the NIH (S10 OD016199). The authors declare no conflict of interests.

We thank the University of Iowa Flow Cytometry Core facility (J. Fishbaugh, H. Vignes, M. Shey, and G. Rasmussen) for cell sorting, and Igor Antoshechkin (California Institute of Technology) for RNA-Seq.

Abbreviations

Tcf1	T cell factor 1
T_{FH}	follicular helper T cells
T_H1	helper 1 T cells
LCMV	lymphocytic choriomeningitis virus

References

1. Harty JT V, Badovinac P. Shaping and reshaping CD8+ T-cell memory. Nature reviews Immunology. 2008; 8:107–119.
2. Chang JT, Wherry EJ, Goldrath AW. Molecular regulation of effector and memory T cell differentiation. Nature immunology. 2014; 15:1104–1115. [PubMed: 25396352]
3. Zhu J, Yamane H, Paul WE. Differentiation of effector CD4 T cell populations (*). Annu Rev Immunol. 2010; 28:445–489. [PubMed: 20192806]
4. Crotty S. T follicular helper cell differentiation, function, and roles in disease. Immunity. 2014; 41:529–542. [PubMed: 25367570]
5. Swain SL, McKinstry KK, Strutt TM. Expanding roles for CD4(+) T cells in immunity to viruses. Nature reviews Immunology. 2012; 12:136–148.
6. Kaech SM, Cui W. Transcriptional control of effector and memory CD8+ T cell differentiation. Nature reviews Immunology. 2012; 12:749–761.
7. Joshi NS, Cui W, Chandele A, Lee HK, Urso DR, Hagman J, Gapin L, Kaech SM. Inflammation directs memory precursor and short-lived effector CD8(+) T cell fates via the graded expression of T-bet transcription factor. Immunity. 2007; 27:281–295. [PubMed: 17723218]
8. Xin A, Masson F, Liao Y, Preston S, Guan T, Gloury R, Olshansky M, Lin JX, Li P, Speed TP, Smyth GK, Ernst M, Leonard WJ, Pellegrini M, Kaech SM, Nutt SL, Shi W, Belz GT, Kallies A. A molecular threshold for effector CD8(+) T cell differentiation controlled by transcription factors Blimp-1 and T-bet. Nature immunology. 2016; 17:422–432. [PubMed: 26950239]
9. Yang CY, Best JA, Knell J, Yang E, Sheridan AD, Jesionek AK, Li HS, Rivera RR, Lind KC, D'Cruz LM, Watowich SS, Murre C, Goldrath AW. The transcriptional regulators Id2 and Id3 control the formation of distinct memory CD8+ T cell subsets. Nature immunology. 2011; 12:1221–1229. [PubMed: 22057289]

10. Ichii H, Sakamoto A, Kuroda Y, Tokuhisa T. Bcl6 acts as an amplifier for the generation and proliferative capacity of central memory CD8+ T cells. J Immunol. 2004; 173:883–891. [PubMed: 15240675]
11. Banerjee A, Gordon SM, Intlekofer AM, Paley MA, Mooney EC, Lindsten T, Wherry EJ, Reiner SL. Cutting edge: The transcription factor eomesodermin enables CD8+ T cells to compete for the memory cell niche. J Immunol. 2010; 185:4988–4992. [PubMed: 20935204]
12. Wu T, Shin HM, Moseman EA, Ji Y, Huang B, Harly C, Sen JM, Berg LJ, Gattinoni L, McGavern DB, Schwartzberg PL. TCF1 Is Required for the T Follicular Helper Cell Response to Viral Infection. Cell reports. 2015
13. Shaw LA, Belanger S, Omilusik KD, Cho S, Scott-Browne JP, Nance JP, Goulding J, Lasorella A, Lu LF, Crotty S, Goldrath AW. Id2 reinforces TH1 differentiation and inhibits E2A to repress TFH differentiation. Nature immunology. 2016; 17:834–843. [PubMed: 27213691]
14. Staal FJ, Sen JM. The canonical Wnt signaling pathway plays an important role in lymphopoiesis and hematopoiesis. Eur J Immunol. 2008; 38:1788–1794. [PubMed: 18581335]
15. Xue HH, Zhao DM. Regulation of mature T cell responses by the Wnt signaling pathway. Annals of the New York Academy of Sciences. 2012; 1247:16–33. [PubMed: 22239649]
16. Zhou X, Yu S, Zhao DM, Harty JT, Badovinac VP, Xue HH. Differentiation and persistence of memory CD8(+) T cells depend on T cell factor 1. Immunity. 2010; 33:229–240. [PubMed: 20727791]
17. Jeannet G, Boudousquie C, Gardiol N, Kang J, Huelsken J, Held W. Essential role of the Wnt pathway effector Tcf-1 for the establishment of functional CD8 T cell memory. Proc Natl Acad Sci U S A. 2010; 107:9777–9782. [PubMed: 20457902]
18. Yu Q, Sharma A, Oh SY, Moon HG, Hossain MZ, Salay TM, Leeds KE, Du H, Wu B, Waterman ML, Zhu Z, Sen JM. T cell factor 1 initiates the T helper type 2 fate by inducing the transcription factor GATA-3 and repressing interferon-gamma. Nature immunology. 2009; 10:992–999. [PubMed: 19648923]
19. Choi YS, Gullicksrud JA, Xing S, Zeng Z, Shan Q, Li F, Love PE, Peng W, Xue HH, Crotty S. LEF-1 and TCF-1 orchestrate TFH differentiation by regulating differentiation circuits upstream of the transcriptional repressor Bcl6. Nature immunology. 2015; 16:980–990. [PubMed: 26214741]
20. Xu L, Cao Y, Xie Z, Huang Q, Bai Q, Yang X, He R, Hao Y, Wang H, Zhao T, Fan Z, Qin A, Ye J, Zhou X, Ye L, Wu Y. The transcription factor TCF-1 initiates the differentiation of TFH cells during acute viral infection. Nature immunology. 2015; 16:991–999. [PubMed: 26214740]
21. Steinke FC, Yu S, Zhou X, He B, Yang W, Zhou B, Kawamoto H, Zhu J, Tan K, Xue HH. TCF-1 and LEF-1 act upstream of Th-POK to promote the CD4(+) T cell fate and interact with Runx3 to silence Cd4 in CD8(+) T cells. Nature immunology. 2014; 15:646–656. [PubMed: 24836425]
22. Xing S, Li F, Zeng Z, Zhao Y, Yu S, Shan Q, Li Y, Phillips FC, Maina PK, Qi HH, Liu C, Zhu J, Pope RM, Musselman CA, Zeng C, Peng W, Xue HH. Tcf1 and Lef1 transcription factors establish CD8(+) T cell identity through intrinsic HDAC activity. Nature immunology. 2016; 17:695–703. [PubMed: 27111144]
23. Xu Z, Xing S, Shan Q, Gullicksrud JA, Bair TB, Du Y, Liu C, Xue HH. Cutting Edge: beta-Catenin-Interacting Tcf1 Isoforms Are Essential for Thymocyte Survival but Dispensable for Thymic Maturation Transitions. J Immunol. 2017; 198:3404–3409. [PubMed: 28348272]
24. Choi YS, Gullicksrud JA, Xing S, Zeng Z, Shan Q, Li F, Love PE, Peng W, Xue HH, Crotty S. LEF-1 and TCF-1 orchestrate T(FH) differentiation by regulating differentiation circuits upstream of the transcriptional repressor Bcl6. Nat Immunol. 2015; 16:980–990. [PubMed: 26214741]
25. Zhao DM, Yu S, Zhou X, Haring JS, Held W, Badovinac VP, Harty JT, Xue HH. Constitutive activation of Wnt signaling favors generation of memory CD8 T cells. J Immunol. 2010; 184:1191–1199. [PubMed: 20026746]
26. Yang Q, Li F, Harly C, Xing S, Ye L, Xia X, Wang H, Wang X, Yu S, Zhou X, Cam M, Xue HH, Bhandoola A. TCF-1 upregulation identifies early innate lymphoid progenitors in the bone marrow. Nature immunology. 2015; 16:1044–1050. [PubMed: 26280998]
27. Zhou X, Xue HH. Cutting edge: generation of memory precursors and functional memory CD8+ T cells depends on T cell factor-1 and lymphoid enhancer-binding factor-1. J Immunol. 2012; 189:2722–2726. [PubMed: 22875805]

28. Lefrancois L, Marzo AL. The descent of memory T-cell subsets. Nature reviews Immunology. 2006; 6:618–623.
29. Johnston RJ, Poholek AC, DiToro D, Yusuf I, Eto D, Barnett B, Dent AL, Craft J, Crotty S. Bcl6 and Blimp-1 are reciprocal and antagonistic regulators of T follicular helper cell differentiation. Science. 2009; 325:1006–1010. [PubMed: 19608860]
30. Hatzi K, Nance JP, Kroenke MA, Bothwell M, Haddad EK, Melnick A, Crotty S. BCL6 orchestrates Tfh cell differentiation via multiple distinct mechanisms. J Exp Med. 2015; 212:539–553. [PubMed: 25824819]
31. Bauquet AT, Jin H, Paterson AM, Mitsdoerffer M, Ho IC, Sharpe AH, Kuchroo VK. The costimulatory molecule ICOS regulates the expression of c-Maf and IL-21 in the development of follicular T helper cells and TH-17 cells. Nature immunology. 2009; 10:167–175. [PubMed: 19098919]
32. Kroenke MA, Eto D, Locci M, Cho M, Davidson T, Haddad EK, Crotty S. Bcl6 and Maf cooperate to instruct human follicular helper CD4 T cell differentiation. J Immunol. 2012; 188:3734–3744. [PubMed: 22427637]
33. Steinke FC, Xue HH. From inception to output, Tcf1 and Lef1 safeguard development of T cells and innate immune cells. Immunol Res. 2014; 59:45–55. [PubMed: 24847765]
34. Lin WW, Nish SA, Yen B, Chen YH, Adams WC, Kratchmarov R, Rothman NJ, Bhandoola A, Xue HH, Reiner SL. CD8+ T Lymphocyte Self-Renewal during Effector Cell Determination. Cell reports. 2016; 17:1773–1782. [PubMed: 27829149]
35. Lin WH, Adams WC, Nish SA, Chen YH, Yen B, Rothman NJ, Kratchmarov R, Okada T, Klein U, Reiner SL. Asymmetric PI3K Signaling Driving Developmental and Regenerative Cell Fate Bifurcation. Cell reports. 2015; 13:2203–2218. [PubMed: 26628372]
36. Nish SA, Zens KD, Kratchmarov R, Lin WW, Adams WC, Chen YH, Yen B, Rothman NJ, Bhandoola A, Xue HH, Farber DL, Reiner SL. CD4+ T cell effector commitment coupled to self-renewal by asymmetric cell divisions. J Exp Med. 2017; 214:39–47. [PubMed: 27923906]
37. Gullicksrud JA, Shan Q, Xue HH. Front Biol. 2017
38. Tubo NJ, Fife BT, Pagan AJ, Kotov DI, Goldberg MF, Jenkins MK. Most microbe-specific naive CD4(+) T cells produce memory cells during infection. Science. 2016; 351:511–514. [PubMed: 26823430]
39. Hale JS, Youngblood B, Latner DR, Mohammed AU, Ye L, Akondy RS, Wu T, Iyer SS, Ahmed R. Distinct memory CD4+ T cells with commitment to T follicular helper- and T helper 1-cell lineages are generated after acute viral infection. Immunity. 2013; 38:805–817. [PubMed: 23583644]
40. Williams MA, Ravkov EV, Bevan MJ. Rapid culling of the CD4+ T cell repertoire in the transition from effector to memory. Immunity. 2008; 28:533–545. [PubMed: 18356084]
41. Tubo NJ, Pagan AJ, Taylor JJ, Nelson RW, Linehan JL, Ertelt JM, Huseby ES, Way SS, Jenkins MK. Single naive CD4+ T cells from a diverse repertoire produce different effector cell types during infection. Cell. 2013; 153:785–796. [PubMed: 23663778]

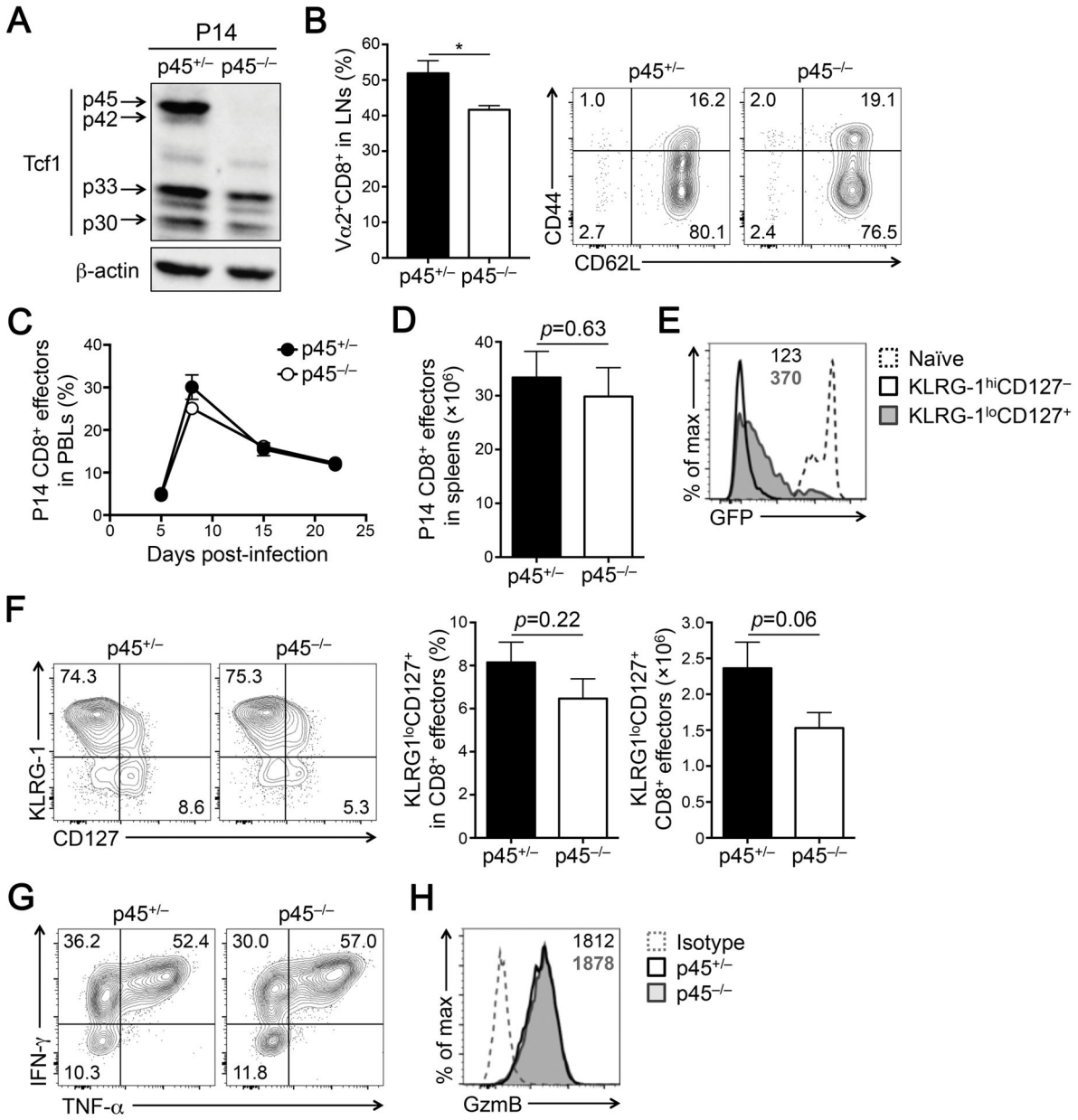

Figure 1. Tcf1 long isoforms are dispensable for effector CD8$^+$ T cell responses

(**A**) Detection of Tcf1 isoforms by immunoblotting in naïve CD8$^+$ T cells. CD62L^{hi}CD44^{lo}Vα2$^+$CD8$^+$ cells were sorted from the LNs of p45$^{+/–}$ or p45$^{–/–}$ P14 transgenic mice and immunoblotted with an anti-Tcf1 or β-actin antibody. (**B**) Characterization of naïve P14 CD8$^+$ T cells. LNs from uninfected p45$^{+/–}$ or p45$^{–/–}$ P14 transgenic mice were surface-stained to detect the frequency (left) and immuno-phenotype (right) of Vα2$^+$CD8$^+$ T cells (n = 4 from 4 experiments). (**C**) Kinetics of CD8$^+$ T cell responses in PBLs. CD45.2$^+$ p45$^{+/–}$ or p45$^{–/–}$ P14 CD8$^+$ T cells (2×10^4 each) were adoptively transferred into CD45.1$^+$ recipients followed by infection with LCMV-Arm. The frequency of CD45.2$^+$ CD8$^+$ effector T cells in CD11a^{hi}CD8^{dim} antigen-experienced CD8$^+$ T cells were monitored in the PBLs on indicated days post-infection (n = 10–20 from 3

experiments). (**D**) Numbers of P14 $CD8^+$ effector T cells detected in the spleen on 8 *dpi* (n = 8 from 3 experiments). (**E**) Detection of Tcf1-EGFP reporter in $p45^{+/-}$ P14 $CD8^+$ effector subsets, and the geometric mean fluorescent intensity (gMFI) of EGFP is marked. Dotted line denotes EGFP expression in naïve $CD8^+$ T cells. (**F**) Detection of P14 $CD8^+$ effector subsets. $CD45.2^+$ $CD8^+$ effector T cells in the spleen (8 *dpi*) were analyzed for KLRG1 and CD127 expression, and the percentages of $KLRG1^{hi}CD127^-$ and $KLRG1^{lo}CD127^+$ subsets are shown in representative contour plots. Cumulative data on the frequency and numbers of the $KLRG1^{lo}CD127^+$ subset are summarized in bar graphs (n = 10 from 3 experiments). (**G**) Cytokine production by P14 $CD8^+$ effector T cells. Splenocytes (8 *dpi*) were incubated with GP33 peptide for 5 hours, and $CD45.2^+CD8^+$ T cells were intracellularly stained to detect IFN-γ and TNF-α. The percentage of each population is shown in representative contour plots from 3 experiments. (**H**) Granzyme B expression in P14 $CD8^+$ effector T cells detected by intracellular staining. gMFI of Granzyme B is shown in representative histogram. Dotted line, isotype control staining. Data in bar graphs are means ± SEM. *, $p < 0.05$ by Student's *t*-test unless specified otherwise.

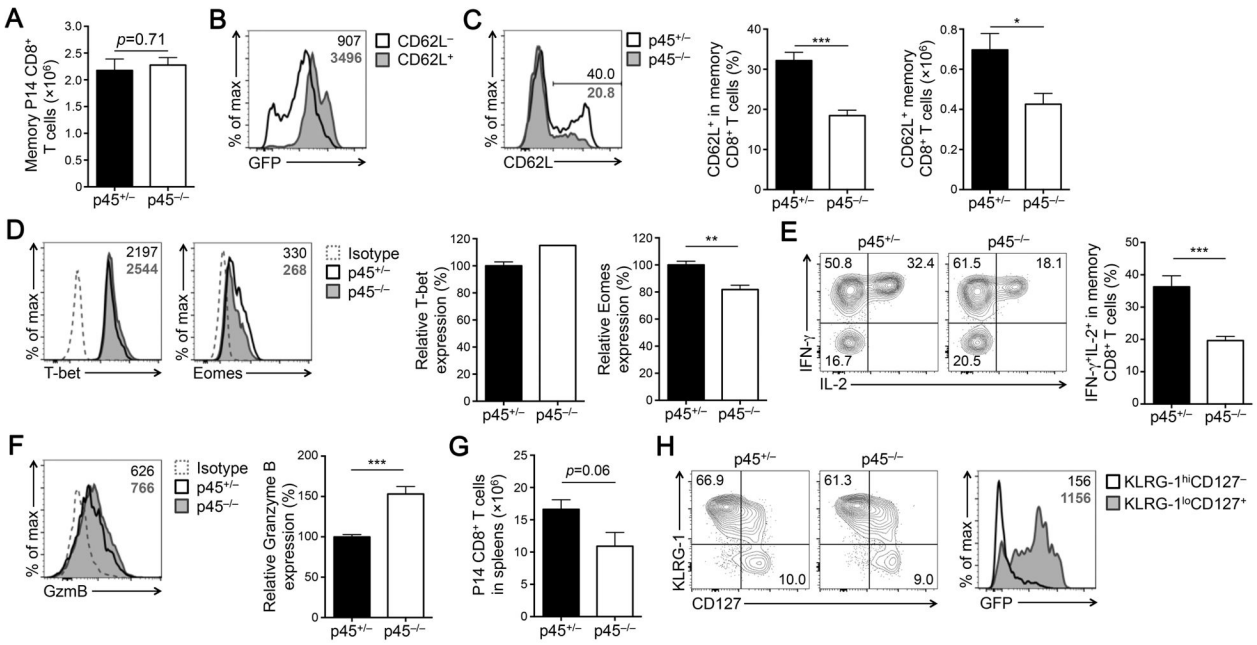

Figure 2. Tcf1 long isoforms contribute to optimal T_{CM} maturation and secondary expansion

(A) Numbers of memory P14 $CD8^+$ T cells detected in the spleen at ≥ 60 *dpi* (n = 5–6 from 2 experiments). **(B)** Detection of Tcf1-EGFP reporter in $CD62L^-$ and $CD62L^+$ memory $CD8^+$ T cell subsets. $CD45.2^+$ memory $CD8^+$ T cells from $p45^{+/-}$ mice were analyzed for EGFP expression, and values in the histogram denote EGFP gMFI. **(C)** Detection of P14 $CD8^+$ T_{CM} cells. $CD45.2^+$ memory $CD8^+$ T cells in the spleen were analyzed for CD62L expression, and the percentages of $CD62L^+$ T_{CM} cells are shown in representative histograms. Cumulative data on the frequency and numbers of the $CD62L^+$ T_{CM} cells are summarized in bar graphs (n = 5–6 from 2 experiments). **(D)** T-bet and Eomes expression in memory P14 $CD8^+$ T cells detected by intranuclear staining. gMFI of T-bet or Eomes is shown in representative histograms, and cumulative data are in bar graphs (for T-bet, n = 2–3 from 1 experiment; for Eomes, n = 5–6 from 2 experiments). Dotted line, isotype control staining. **(E)** Cytokine production by memory P14 $CD8^+$ T cells. Splenocytes were harvested at ≥ 60 *dpi* and incubated with GP33 peptide, followed by intracellular detection of IFN-γ and IL-2 in $CD45.2^+CD8^+$ T cells. The percentage of each population is shown in representative contour plots (n = 8 from 3 experiments), and that of IFN-γ– and IL-2-double producers are summarized in bar graphs. **(F)** Granzyme B expression in memory P14 $CD8^+$ T cells detected by intracellular staining. gMFI of Granzyme B is shown in representative histogram, and cumulative data are in bar graphs (n = 8 from 3 experiments). Dotted line, isotype control staining. **(G)** Numbers of secondary $CD8^+$ effector T cells. The immune $CD45.1^+$ recipients were infected with LCMV-Cl13, and five days after infection, the numbers of $CD45.2^+CD8^+$ secondary effector T cells were determined in the spleen (n = 5 from 2 experiments). **(H)** Characterization of P14 $CD8^+$ secondary effector T cells. $CD45.2^+CD8^+$ secondary effector T cells in the spleen were surface-stained, and the percentages of $KLRG1^{hi}CD127^-$ and $KLRG1^{lo}CD127^+$ subsets are shown in representative contour plots (left panels). Both subsets were analyzed for Tcf1-EGFP reporter expression in $p45^{+/-}$ recipients, with EGFP gMFI marked (right panel, n = 5–6 from 2 experiments). Data

in bar graphs are means ± SEM. *, $p < 0.05$; **, p<0.01; ***, $p < 0.001$ by Student's *t*-test unless specified otherwise.

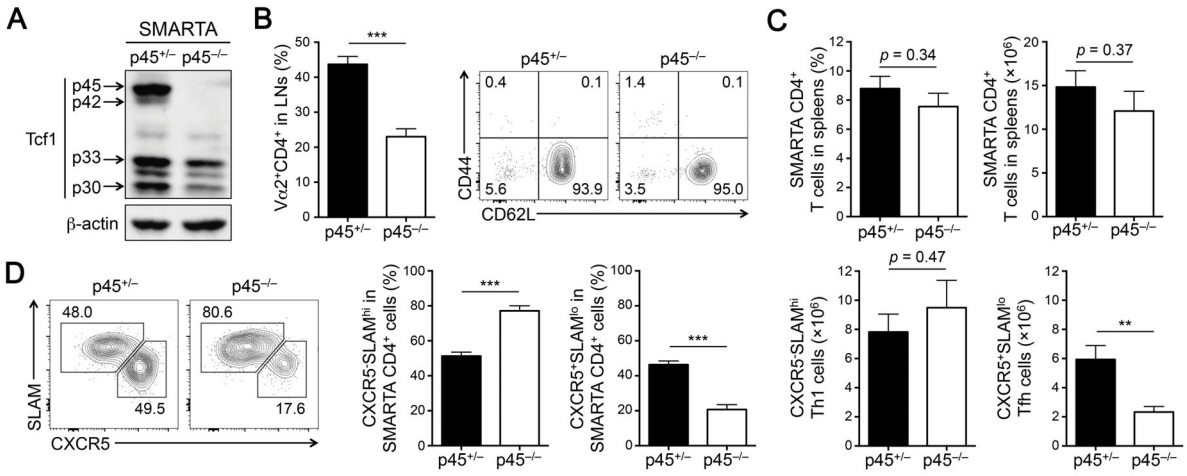

Figure 3. Tcf1 long isoforms regulate optimal T_{FH} differentiation

(A) Detection of Tcf1 isoforms by immunoblotting in $CD4^+$ T cells. $CD62L^{hi}CD44^{lo}V\alpha2^+CD4^+$ cells were sorted from the LNs of $p45^{+/-}$ or $p45^{-/-}$ SMARTA-Tg mice and immunoblotted as in Figure 1A. **(B)** Characterization of naïve SMARTA $CD4^+$ T cells. LNs were isolated from $p45^{+/-}$ or $p45^{-/-}$ SMARTA-Tg mice and surface-stained to detect the frequency (left) and immunophenotype (right) of $V\alpha2^+CD4^+$ T cells (n = 8 from 8 experiments). **(C)** Detection of effector SMARTA $CD4^+$ T cells at the peak response. $CD45.2^+$ $p45^{+/-}$ or $p45^{-/-}$ SMARTA $CD4^+$ T cells from LN (2×10^5 each) were adoptively transferred into $CD45.1^+$ recipients followed by infection with LCMV-Arm. On 8 *dpi*, $CD45.2^+CD4^+$ T cells were detected and enumerated in the spleens of recipient mice (n = 8 from 3 experiments). **(D)** Detection of T_H1 and T_{FH} effector $CD4^+$ T cells. $CD45.2^+$ effector $CD4^+$ T cells (as in **C**) were analyzed for CXCR5 and SLAM expression. The percentages of $CXCR5^-SLAM^{hi}$ T_H1 and $CXCR5^+SLAM^{lo}$ T_{FH} cells are shown in representative contour plots (left panels). Cumulative data on the frequency and numbers of each subset are summarized in bar graphs (n = 5–8 from 2–3 experiments). Data are means ± SEM. **, $p < 0.01$; ***, $p < 0.001$ by Student's *t*-test unless specified otherwise.

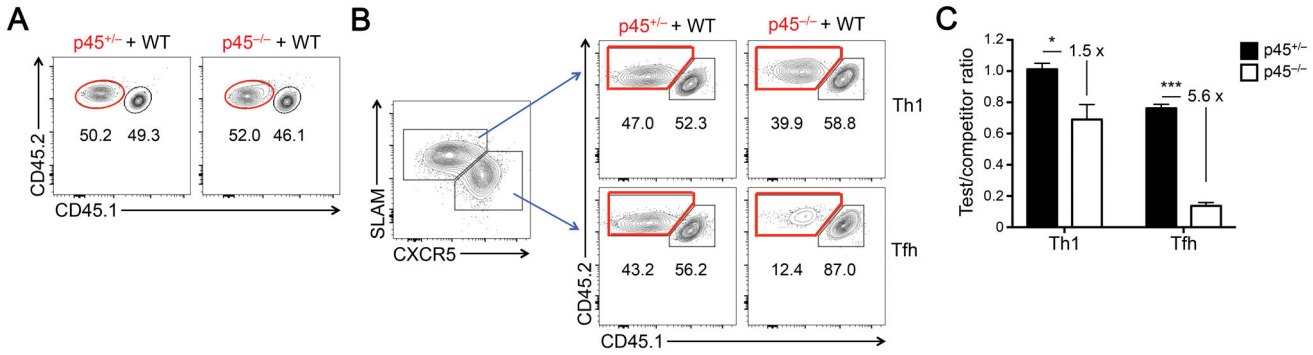

Figure 4. CD4$^+$ T cells lacking Tcf1 long isoforms are less competitive in T_{FH} differentiation

(A) Relative abundance of CD45.2$^+$ test cells (p45$^{+/-}$ or p45$^{-/-}$) and CD45.1$^+$CD45.2$^+$ competitors (WT CD4$^+$ T cells) in the cell mixture used in competitive transfer experiments. **(B)** Detection of relative contribution of test and competitor SMARTA CD4$^+$ T cells to T_H1 and T_{FH} responses. CXCR5$^-$SLAM^{hi} T_H1 cells and CXCR5$^+$SLAM^{lo} T_{FH} cells were detected in the recipients on 8 *dpi* (left). Within each subset, the percentages of test and competitor cells were determined and shown in representative contour plots. **(C)** Cumulative data of test/competitor ratio within T_H1 or T_{FH} subsets at the effector phase (8 *dpi*). Data are from 2 experiments (n = 5–6). Data are means ± SEM. *, $p < 0.05$; ***, $p < 0.001$ by Student's *t*-test.

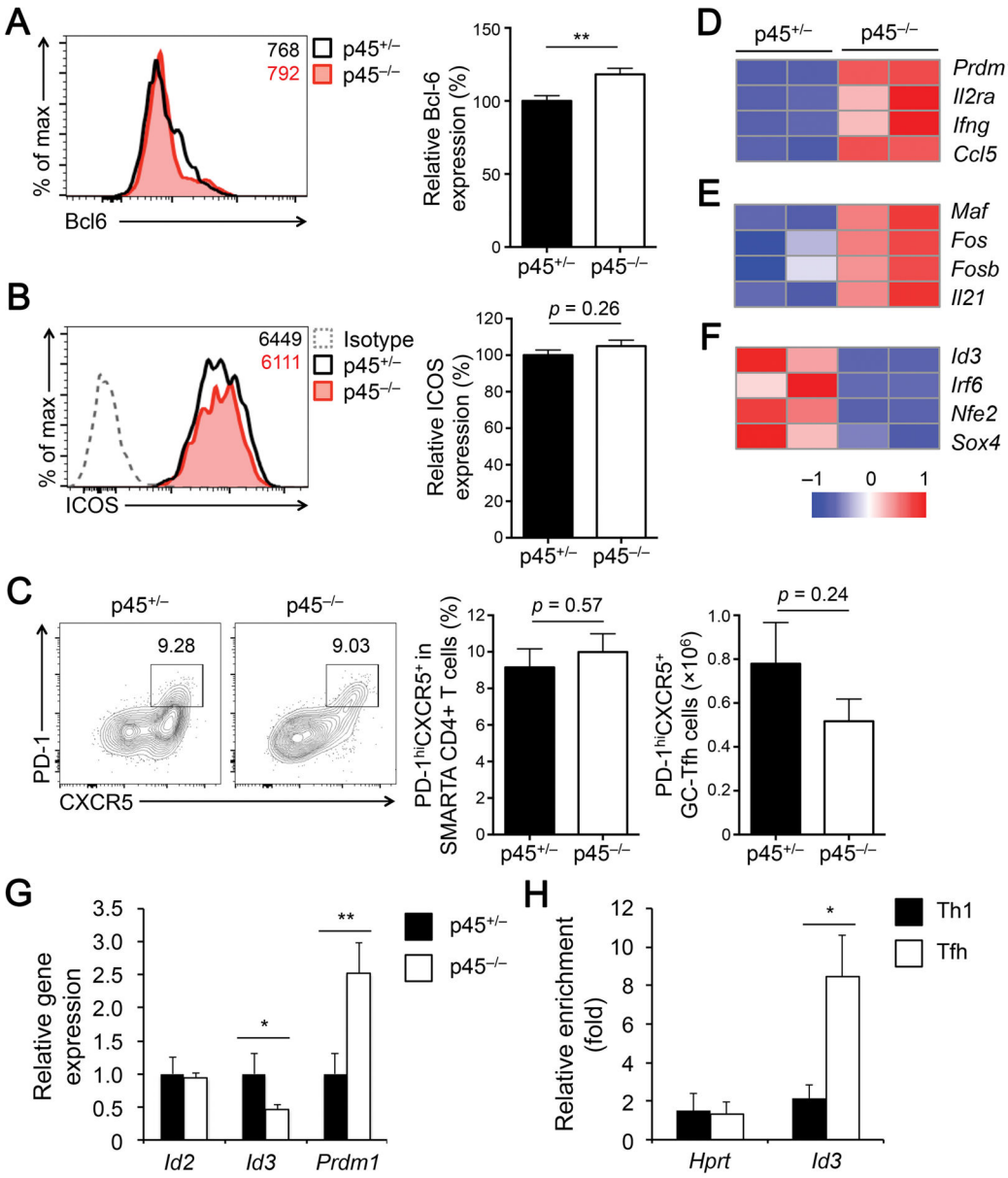

Figure 5. Tcf1 long isoforms are essential for regulating a subset of T_{FH} transcriptional program

(A–B) Detection of Bcl6 (**A**) and ICOS **(B)** in $p45^{+/-}$ and $p45^{-/-}$ $CXCR5^+SLAM^{lo}$ T_{FH} cells (8 *dpi*). gMFI of each protein is shown in representative histograms, and cumulative data on the relative expression between $p45^{+/-}$ and $p45^{-/-}$ T_{FH} cells are in bar graphs (n = 11 from 4 experiments). (**C**) Detection of PD-$1^{hi}CXCR5^+$ GC-T_{FH} cells (8 *dpi*). The percentages of GC-T_{FH} cells among $CD45.2^+$ SMARTA $CD4^+$ T cells are shown in representative contour plots, and cumulative data in bar graph are from 2 experiment (n = 6). (**D–F**) Heatmaps of select differentially expressed genes. $p45^{+/-}$ and $p45^{-/-}$ PD-$1^{lo}CXCR5^+$ non-GC T_{FH} cells were sorted from splenic $CD45.2^+$ SMARTA $CD4^+$ T cells in the recipients on 8 *dpi*. Two biological replicates were collected for each genotype and analyzed with RNA-Seq. (**G**) Detection of select gene expression in non-GC T_{FH} cells by quantitative RT-PCR. The cells

were sorted using the same strategy as above. For each gene of interest, its expression in $p45^{+/-}$ cells was set as 1, and its relative expression in $p45^{-/-}$ cells was calculated accordingly. Data are from two independent experiments (n = 3–4). (**H**) Detection of enriched Tcf1 binding. WT T_H1 and T_{FH} cells were sorted and subjected to ChIP analysis. The relative enrichment at the control *Hprt* locus and *Id3* transcription start site by an anti-Tcf1 antibody was determined by quantitative PCR. Data are from two independent experiments with each sample measured in duplicates or triplicates. Data in bar graphs are means ± SEM. *, $p < 0.05$; **, $p < 0.01$ by Student's *t*-test unless specified otherwise.

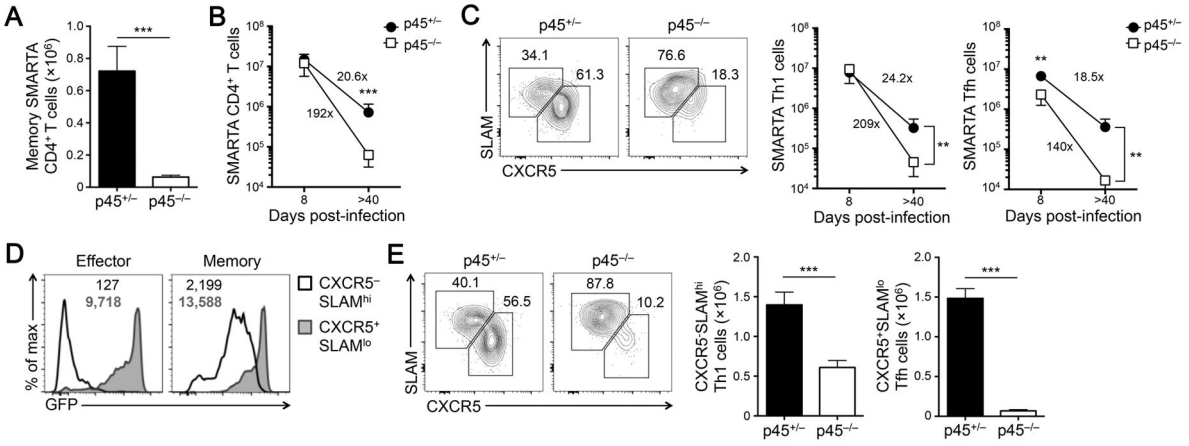

Figure 6. Tcf1 long isoforms are critical for formation of memory T_H1 and memory T_{FH} cells

(A) Detection of memory SMARTA $CD4^+$ T cells. Adoptive transfer and infection were performed as in Figure 3. On >40 *dpi*, $CD45.2^+CD4^+$ T cells were detected and enumerated in the spleens of recipient mice (n = 7–8 from 3 experiments). **(B)** Population fold changes due to contraction. $p45^{+/-}$ and $p45^{-/-}$ SMARTA $CD4^+$ T cells were enumerated at the peak (8 *dpi*) and memory (> 40 *dpi*) phases in response to viral infection, and fold reduction between the two phases is calculated (n = 8 from 3 experiments). **(C)** Detection of memory T_H1 and T_{FH} T cells. $CD45.2^+CD4^+$ T cells were analyzed for CXCR5 and SLAM expression. The percentages of $CXCR5^-SLAM^{hi}$ memory T_H1 and $CXCR5^+SLAM^{lo}$ memory T_{FH} cells are shown in representative contour plots (left panels). Cumulative data on the numbers of T_H1 and T_{FH} cells at both effector and memory phases are summarized in line graphs (right panels), and the fold reduction during contraction of each cell type is calculated (n = 8 from 3 experiments). **(D)** Detection of Tcf1-EGFP reporter in $CXCR5^-SLAM^{hi}$ T_H1 and $CXCR5^+SLAM^{lo}$ T_{FH} cells. $p45^{+/-}$ T_H1 and T_{FH} cells at the effector (8 *dpi*, left) and memory (>40 *dpi*, right) phases were analyzed for EGFP expression, and values in the histograms denote EGFP gMFI. **(E)** Detection of secondary T_H1 and T_{FH} effector responses. The immune $CD45.1^+$ recipients were infected with LCMV-Cl13 and five days later, $CD45.2^+$ secondary T_H1 and T_{FH} effector T cells were detected in the spleen. The frequency of each subset is shown in representative contour plots, and the cumulative data on cell numbers are summarized in bar graphs (n =6–8 from 3 experiments). Data are means ± SEM. For all paired comparison, **, $p < 0.01$; ***, $p < 0.001$ by Student's *t*-test.